

# Optimal Seismic Reflectivity Inversion: Data-driven $\ell_p$ -loss- $\ell_q$ -regularization Sparse Regression

Fangyu Li, Rui Xie, *Student Member, IEEE*, Wen-Zhan Song, *Senior Member, IEEE*, Hui Chen

**Abstract**—Seismic reflectivity inversion is widely applied to improve the seismic resolution to obtain detailed underground understandings. Based on the convolution model, seismic inversion removes the wavelet effect by solving an optimization problem. Taking advantage of the sparsity property, the  $\ell_1$  norm is commonly adopted in the regularization terms to overcome the noise/interference vulnerability observed in the  $\ell_p$ -losses minimization. However, no one has provided a deterministic conclusion that  $\ell_1$  norm regularization is the best choice for seismic reflectivity inversion. Instead of using an unproved fixed regularization norm, we propose an optimal seismic reflectivity inversion approach. Our method adaptively adopts a  $\ell_p$ -loss- $\ell_q$ -regularization (i.e.  $\ell_{p,q}$  regularization) for  $p = 2$ ,  $0 < q < 1$  to estimate a more accurate and detailed reflectivity profile. In addition, we employ a  $K$  fold cross-validation based approach to obtain the optimal damping factor  $\lambda$  to further improve the seismic inversion results. The letter starts with the introduction of non-convex constraint for seismic inversion, and the necessity of the  $\ell_q$  norm regularization. Then the majorization-minimization and cross validation algorithms are briefly described. The performance of the proposed seismic inversion approach is evaluated through synthetic examples and a field example from the Bohai Bay Basin, China.

**Index Terms**—seismic reflectivity inversion,  $\ell_{p,q}$  regularization, damping factor, cross-validation, optimal regularization.

## I. INTRODUCTION

**R**ESOLUTION is an unavoidable topic in seismic interpretation, which is the ultimate goal for all seismic processing steps. High seismic resolution helps characterizing the correlation between the geological structures and geophysical images, which is important for the reservoir deposition analysis, especially thin-bed reservoirs [1].

Based on the seismic convolution model, [2] improved the seismic resolution via a wavelet scaling method. Likewise, [3] extended seismic spectrum using a non-stationary wavelet estimation. A seismic reflectivity obtained from seismic amplitude inversion has been used in the applications with little/weak well controls [4]. For regularized inversion, besides the  $\ell_2$  norm constraint,  $\ell_1$  norm regularization is more popular in sparse spike inversion [5], [6]. Theoretically,  $\ell_0$  norm regularization should also be a good sparsity measurement, but actual seismic signals do not always show 0 values, so

finding exact  $p$  non-zero elements in signal, i.e.  $\|x\|_0 = p$  is not a computationally feasible and proper constraint in the real world [7]. Signal sparsity properties show different highlights [8], so a data-driven sparsity measurement is more suitable for the seismic reflectivity inversion problem [9], [10]. The convergence of  $\ell_q$  ( $0 < q < 1$ ) norm regularization has been proved by [11], and its advantages were also demonstrated. There are some well established algorithms to solve the nonconvex or concave optimization problem related to  $\ell_q$  regularized inversion, for examples, cyclic descent algorithm [12], reweighted  $\ell_1$  minimization [13], iteratively reweighted algorithms [14], and so on.

However, to our best knowledge, the sparsity regularization selection for seismic reflectivity inversion has not been generally discussed. Although there are discussions with the damping factor  $\lambda$  selection, such as [10], they are only related to either  $\ell_1$  or  $\ell_2$  norm. In the previous work [15], a  $\ell_q$  norm ( $0 < q < 1$ ) regularized optimization has been applied to the seismic reflectivity inversion. Compared to [15], this letter proposes a general data-driven seismic reflectivity inversion approach. We extend  $\ell_q$  norm ( $0 < q < 1$ ) norm to a  $\ell_p$ -loss- $\ell_q$ -regularization ( $\ell_{p,q}$  regularization) framework, which allows us to consider a wide range of loss functions. The possible choices of loss functions include the  $\ell_p$ -losses and prediction losses [11]. In this letter, we study the  $\ell_2$ -loss as an illustration. Here, we also explicitly define the way to obtain the optimal  $q$ , where the majorize-minimization (MM) algorithm is described. In addition,  $K$  fold cross-validation is adopted for generality. We establish an adaptive seismic inversion approach including optimal regularization term selection as well as adaptive damping factor determination. We introduce the theories and algorithms first. Then effectiveness of the proposed method is proved through synthetic examples and a field application from Bohai Bay Basin, China.

## II. THEORY

### A. Seismic Convolution Model

After removing the undesirable interferences, seismic data can be modeled as the convolution between the source wavelet  $w(t)$  and reflectivity series  $r(t)$  in the form as [10], [15], [16]:

$$s(t) = \int_{-\infty}^{\infty} w(\tau)r(t - \tau)d\tau + \epsilon(t), \quad (1)$$

where  $\epsilon(t)$  is an additive random noise. Using a convolution symbol, we can rewrite it as:

$$s(t) = w(t) * r(t) + \epsilon(t). \quad (2)$$

Manuscript received August xx, 2018.

The research is partially supported by NSF-CNS-1066391, NSF-CNS-0914371, NSF-CPS-1135814, NSF-CDI-1125165, NSF-DMS-1222718, NIH-R01GM122080, NIH-R01GM113242 and Southern Company.

F. Li, R. Xie and W. Song are with University of Georgia, Athens, GA 30602, USA e-mail: (fangyu.li@uga.edu; ruixie@uga.edu; wsong@uga.edu)

H. Chen is with Geomathematics Key Laboratory of Sichuan Province, Chengdu University of Technology, Chengdu, China, e-mail: (huichendut@cdut.edu.cn)

Then, a discrete matrix format realized at samples  $t = 1, 2, \dots, M$  can also be formulated [17]:

$$\mathbf{s} = \mathbf{W}\mathbf{r} + \mathbf{e}, \quad (3)$$

where  $\mathbf{s} = [s_1, \dots, s_M]^T$  is the observation,  $\mathbf{W}$  is the wavelet kernel matrix which can be estimated from the seismic power spectrum [16], and  $\mathbf{r} = [r_1, \dots, r_M]^T$  is the reflectivity series.

### B. Seismic Inversion

The seismic convolution model forms a linear relationship between the recorded seismic data and reflectivity series. The solution of equation (3) is nonunique, which necessitates certain constraint to achieve stable. In general, the objective function can be formulated as

$$\phi(q, \lambda) = \|\mathbf{s} - \mathbf{W}\mathbf{r}\|_p^p + \lambda \|\mathbf{r}\|_q, \quad (4)$$

where  $\|\mathbf{s} - \mathbf{W}\mathbf{r}\|_p^p = \sum_{t=1}^M |s(t) - w(t) * r(t)|_p^p$  and  $\|\mathbf{r}\|_q = (\sum_{j=1}^M |r_j|^q)^{1/q}$  ( $q$  indicates the constraint condition) and  $\lambda$  is the damping factor [12]. The common choice for the loss function is the  $\ell_2$ -loss, i.e.  $p=2$ .

### C. $\ell_q$ Norm Regularization

Seismic inversion usually adopts either  $\ell_1$  or  $\ell_2$  norm regularization. This nonconvex constraint is based on the common assumption that the reflectivity series  $r(t)$  is sparse. However, accurately identifying the sparsity of the signal is not easy. The  $\ell_0$  norm, which measures the number of non-zero of  $\mathbf{r}$ :  $\|\mathbf{r}\|_0 = \{r_j \neq 0, j = 1, \dots, N\}$ , is not put into consideration. It asks to find the “best subset” among all possible sparsity candidates that makes it impractical for seismic reflectivity due to intractable computational cost and difficulty in choosing number of non-zero elements. To loose the constraint, the  $\ell_1$  norm regularization, i.e. Lasso regression [18], is easily calculated with sparsity constraint. [19] built the connection between  $\ell_0$  and  $\ell_2$  regularization. Because the convex  $\ell_q$  regularization with  $q > 1$  does not hold the sparsity property which is necessary for seismic inversion, we need to pick an optimal  $q$  from  $(0, 1)$ . As shown in Figure 1, different regularization norms produce various constraint on sparsity.

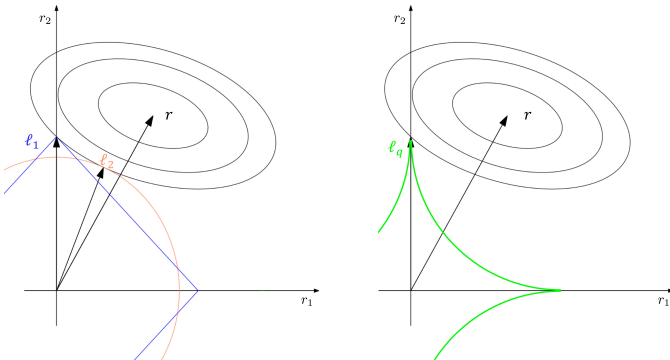


Fig. 1. Geometric interpretation of different regularizations. Left:  $\ell_1$  regularization (blue),  $\ell_2$  regularization (red); Right:  $\ell_q$  (green) regularization with  $q = 0.5$ . The ellipses are contours of the  $\ell_p$ -loss errors of the toy signal  $\mathbf{r} = [r_1, r_2]^T$ .

In order to obtain the optimal choice of  $q$ , for a given  $\lambda$ , we can formulate the objective function as:

$$\hat{q} = \arg \min_{q \in \mathcal{Q}} \phi(q, \lambda) \Rightarrow \hat{q} = \arg \min_{q \in \mathcal{Q}} \phi(q), \quad (5)$$

where  $\mathcal{Q}$  is a predefined nonempty set containing possible  $q$  values. This problem can be solved through a coordinate-wise optimization method.

### D. Majorize-Minimization Algorithm

We propose to use the majorize-minimization (MM) algorithm [20] to solve the nonconvex optimization problem in equation (4) with  $0 < q < 1$ . As an iterative optimization method, the MM algorithm consists of two steps in one iteration. In the first majorization step, a surrogate function  $g(\cdot|q_k)$  is employed to locally approximate the objective function with their difference minimized at the current point. In other words, the surrogate upperbounds the objective function up to a constant  $c_k$ . Then in the minimization step, the surrogate function is minimized. The sequence  $\phi(q_k)$  is non-increasing since  $\phi(q_{k+1}) \leq g(q_{k+1}|q_k) - c_k \leq g(q_k|q_k) - c_k = \phi(q_k)$ . The procedure is shown in Algorithm 1. The computational complexity of the MM algorithm is  $O(M^3)$ .

---

#### Algorithm 1: Majorization-Minimization Algorithm

---

- 1: Initialize  $q_0 \in \mathcal{Q}$  and set  $k = 0$
  - 2: **repeat**
  - 3:   **Majorization step:**
  - 4:   Construct  $g(\cdot|q_k)$  satisfying the upperbound property:  $g(q|q_k) \geq \phi(q) + c_k, \forall q \in \mathcal{Q}$
  - 5:   **Minimization step:**
  - 6:   Update  $x$  as  $q_{k+1} = \arg \min_{q \in \mathcal{Q}} g(q|q_k)$
  - 7:    $k \leftarrow k + 1$
  - 8: **until** certain convergence criterion is met
- 

### E. Damping Factor Selection

The damping factor  $\lambda$  in equation (4) controls the sparsity of the recovered signal. We propose to use the cross-validation (CV) [21] approach to choose the optimal value of damping factor, which works for parameter selection according to its statistical performance. Cross-validation provides the optimal bias-variance tradeoff under the setting of equation (4). The  $K$ -fold CV is adopted roughly as: First, randomly split the data into  $K$  equal clusters; Second, the  $k$ th cluster ( $k = 1, 2, \dots, K$ ) is used for testing the optimization model fitted using the data from other cluster; Third, the CV prediction error for each  $\lambda$  is calculated; Then, repeat the random selection; In the end, combine all the  $K$  prediction errors together to obtain the CV estimate:

$$CV(\lambda) = \frac{1}{K} \sum_{k=1}^K \left( \mathbf{s}_k - \mathbf{W}_k \hat{\mathbf{r}}^{(-k)}(\lambda) \right)^2, \quad (6)$$

leading to the chosen optimal  $\hat{\lambda} = \arg \min_{\lambda \in [a, b]} CV(\lambda)$ , where  $[a, b]$ ,  $a, b \in \mathbb{R}_+$  is the given range of  $\lambda$ .

### III. EXPERIMENTS

#### A. Synthetic Example

We first test the proposed method in numerical experiments. Compared with synthetic experiments in [10] and [15], we designed the sparse reflectivity series randomly instead of using fixed positions, which makes more sense for the non-stationary seismic applications.

Table I shows the comparisons of the similarity measurement between ground truth and inverted reflectivity with different SNRs.  $\ell_2$ ,  $\ell_1$  and  $\ell_{p,q}$  regularizations are applied to invert the random reflectivity profile, respectively. SNR varies from 20 dB to -10 dB, which covers possible SNR situations of field applications. And Monte-Carlo experiments are conducted 100 times for every different situation. Note that the proposed  $\ell_{p,q}$  method achieves the highest inversion accuracies at different noise levels with relatively stable performances. Specifically, when the data have a low SNR, the proposed regularization constraint produces the most robust results.

TABLE I. Similarity between the ground truth and inverted reflectivity profile from 100 times Monte-Carlo experiments of every situation. ('std' stands for standard deviation.)

SNR (dB)	Regularization					
	$\ell_2$		$\ell_1$		$\ell_{p,q}$	
	mean	std	mean	std	mean	std
20	0.5038	0.0625	0.8602	0.0402	0.8624	0.0424
10	0.4991	0.0726	0.8362	0.0426	0.8541	0.0453
3	0.4701	0.0670	0.8081	0.0492	0.8279	0.0473
0	0.4292	0.0650	0.7896	0.0564	0.7981	0.0556
-3	0.3914	0.0694	0.7417	0.0738	0.7840	0.0584
-10	0.3685	0.0690	0.5156	0.1865	0.7385	0.0737

To visualize the results, Figure 2(a) shows one of synthetic Monte-Carlo reflectivity models consisting of randomly located, sparse reflectivity series. Based on the convolution model, we obtain the seismic data by convolving the reflectivity profile with a 30 Hz Ricker wavelet. The synthetic seismic trace is shown in Figure 2(b). Figure 2(c) displays a noisy seismic trace with 10 dB random noise. Figures 2(d)-2(f) demonstrate the inverted results from the noisy seismic data based on the regularizations of  $\ell_2$ ,  $\ell_1$  and proposed  $\ell_q$  norms. Our proposed  $\ell_q$  method and  $\ell_1$  norm successfully recovered the sparsity of the reflectivity, where  $\ell_2$  norm failed to do so. Compared to  $\ell_1$  norm, the proposed  $\ell_q$  method captured more detailed information, such as small-amplitude picks, successive picks, than  $\ell_1$  norm method. Due to the highly non-convexity of the  $\ell_q$  regularization, our proposed method distinguishes the true non-zero reflectivity components from noises by projected observed data onto a  $\ell_q$ -ball. By searching the  $\ell_q$ -ball using MM algorithm, the true reflectivity can be efficiently recovered from the noisy data. The results demonstrated that, under the noise contamination, the  $\ell_q$  method outperforms the popular seismic inversion techniques such as  $\ell_1$  or  $\ell_2$  norm regularized inversion.

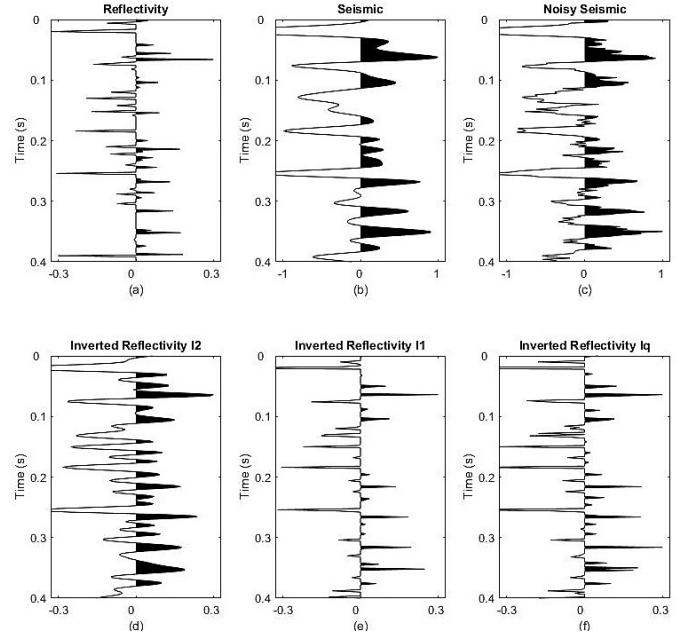


Fig. 2. Synthetic example. (a) Random reflectivity; (b) Synthetic seismic trace; (c) Noisy seismic trace with 10 dB noise; And Inverted reflectivity from (d)  $\ell_2$  norm, (e)  $\ell_1$  norm and (f) the proposed  $\ell_q$  method.

#### B. Field Application

We apply the proposed method to seismic field data from Bohai Bay Basin, China. The target reservoir in this area is the siliciclastic reservoir, where the thin bed structure develops, so the high resolution interpretation, especially the reflectivity inversion is of great importance.

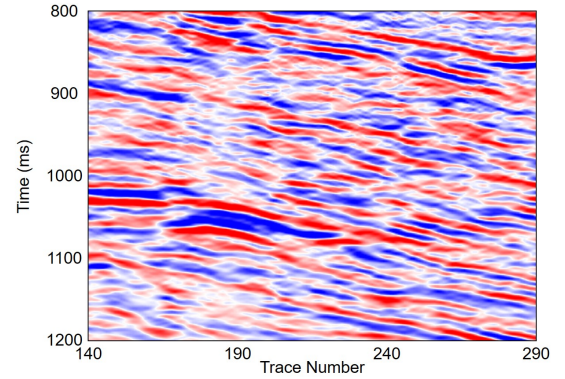


Fig. 3. Field seismic data from Bohai Bay Basin, China.

We display the original seismic amplitude in Figure 3. Figure 4 is the inverse result of  $\ell_2$  norm regularization with 5-fold CV. We see that it fails to remove the noise from observations or recover the sparse reflectivity series. Compared to  $\ell_2$  method,  $\ell_1$  and  $\ell_q$  methods shown in Figure 5-7 provide more sparse recovered reflectivity series. The optimal  $\ell_q$  inverse result with  $q = 0.7$  is shown in Figure 6. We see that our proposed  $\ell_q$  method recovered more detailed information when comparing to the  $\ell_1$  method, and more thin beds can



be characterized now. Note that the damping factors for both methods are chosen using 5-fold CV.

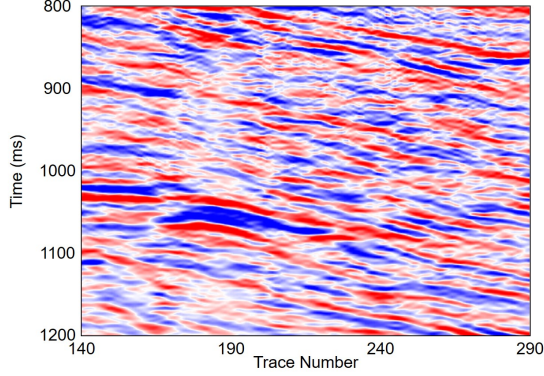


Fig. 4. Seismic inversion using  $\ell_2$  norm.

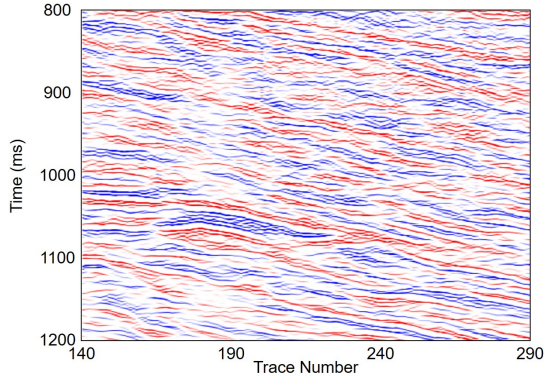


Fig. 5. Seismic inversion using  $\ell_1$  norm.

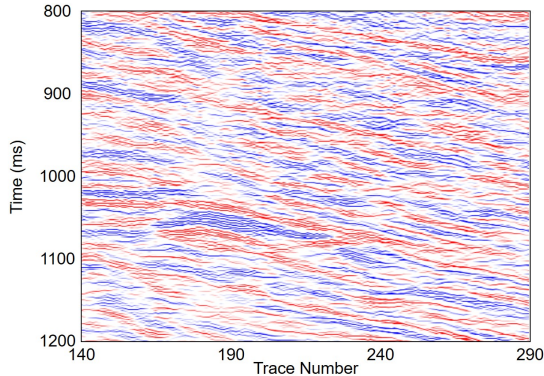


Fig. 6. Seismic inversion using  $\ell_q$  norm.

To demonstrate the effectiveness of choice of damping factors, we compare the optimal  $\ell_q$  inversion (Figure 6) with an over regularized  $\ell_q$  inversion (Figure 7). We see that a proper regularization, i.e. finding optimal damping factor using CV, will help keeping the continuity of the inversion result while maintaining the sparsity.

To further evaluate the inverted results, we compare the  $\ell_1$  and  $\ell_q$  norm inversion reflectivity profiles with the reflectivity calculated from the sonic logs, shown in Figure 8. The results from the proposed  $\ell_q$  norm inversion show more details and have better correspondence with the reflectivity from well

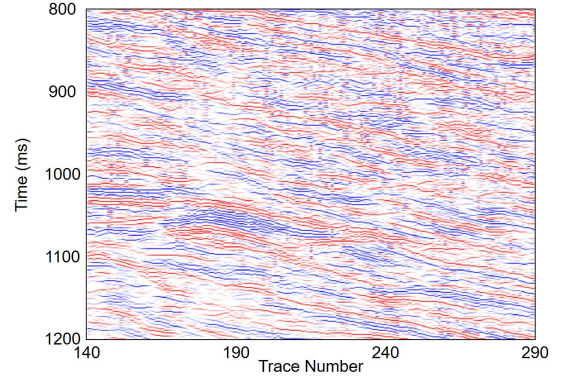


Fig. 7. Seismic inversion using  $\ell_q$  norm without optimal regularization parameter selection.

logs. In addition, we also calculate the relative similarity coefficient,  $\rho(\cdot, \text{Refl}_{\log}) / \rho(\text{Seismic}, \text{Refl}_{\log})$ , between the inverted reflectivity and the sonic reflectivity with  $\rho(\cdot)$  as the cross correlation function, which are 0.5843 with the  $\ell_q$  norm and 0.4347 with the  $\ell_1$  norm. So from both qualitative and quantitative comparisons, the proposed method is better than the existing methods.

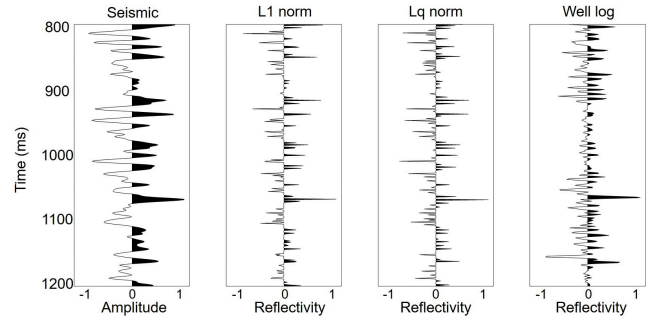


Fig. 8. Comparison among the reflectivity calculated from the sonic logs, the inverted reflectivity based on  $\ell_1$  and  $\ell_q$  norms. (The trace number is 209.)

#### IV. CONCLUSIONS

We propose a novel sparse reflectivity inversion method with  $\ell_{p,q}$  norm regularization and optimal damping factor selection. The non-convex constraints have drawn a lot of attentions, because it satisfies the mathematical assumptions of seismic reflectivity series. Illustrating the case of  $p = 2$ , we adaptively adopt the  $\ell_q$  ( $0 < q < 1$ ) norm constraint. In addition, because the estimates of  $q$  and  $\lambda$  value are fully data-driven, we believe the inverted results are relatively optimal. The synthetic examples verify that the proposed method can eliminate the effects of wavelet effectively and can obtain the stable reflectivity series even with moderate random noises. Furthermore, the derived reflectivity in the field example shows high correspondence with the reflectivity calculated from well logs.

## REFERENCES

- [1] B. A. Kurniawan, E. Z. Naeini, and D. Kazyyeva, "Spectral decomposition based inversion: application on brenda field, central north sea basin," *First Break*, vol. 31, no. 10, pp. 83–92, 2013.
- [2] S. Chen and Y. Wang, "Seismic resolution enhancement by frequency-dependent wavelet scaling," *IEEE Geoscience and Remote Sensing Letters*, 2018.
- [3] H. Zhou, Y. Wang, T. Lin, F. Li, and K. J. Marfurt, "Value of nonstationary wavelet spectral balancing in mapping a faulted fluvial system, bohai gulf, china," *Interpretation*, vol. 3, no. 3, pp. SS1–SS13, 2015.
- [4] C. R. Conti, M. Roisenberg, G. S. Neto, and M. J. Porsani, "Fast seismic inversion methods using ant colony optimization algorithm," *IEEE Geoscience and Remote Sensing Letters*, vol. 10, no. 5, pp. 1119–1123, 2013.
- [5] L. Liu and W. Lu, "A fast  $l_1$  linear estimator and its application on predictive deconvolution," *IEEE Geoscience and Remote Sensing Letters*, vol. 12, no. 5, pp. 1056–1060, 2015.
- [6] G. Zhang and J. Gao, "Inversion-driven attenuation compensation using synchrosqueezing transform," *IEEE Geoscience and Remote Sensing Letters*, vol. 15, no. 1, pp. 132–136, 2018.
- [7] M. E. Lopes, "Unknown sparsity in compressed sensing: denoising and inference," *IEEE Transactions on Information Theory*, vol. 62, no. 9, pp. 5145–5166, 2016.
- [8] N. Hurley and S. Rickard, "Comparing measures of sparsity," *IEEE Transactions on Information Theory*, vol. 55, no. 10, pp. 4723–4741, 2009.
- [9] J. Ma, H. Zhou, J. Zhao, Y. Gao, J. Jiang, and J. Tian, "Robust feature matching for remote sensing image registration via locally linear transforming," *IEEE Transactions on Geoscience and Remote Sensing*, vol. 53, no. 12, pp. 6469–6481, 2015.
- [10] B. Wang, Z. Guo, X. Chen, and W. Lu, "Nonstationary sparse-reflectivity inversion using nonconvex constraint in frequency domain," in *SEG Technical Program Expanded Abstracts 2016*. Society of Exploration Geophysicists, 2016, pp. 3741–3745.
- [11] G. Raskutti, M. J. Wainwright, and B. Yu, "Minimax rates of estimation for high-dimensional linear regression over  $\ell_q$ -balls," *IEEE transactions on information theory*, vol. 57, no. 10, pp. 6976–6994, 2011.
- [12] G. Marjanovic and V. Solo, " $l_{-q}$  sparsity penalized linear regression with cyclic descent," *IEEE Transactions on Signal Processing*, vol. 62, no. 6, pp. 1464–1475, 2014.
- [13] E. J. Candes, M. B. Wakin, and S. P. Boyd, "Enhancing sparsity by reweighted  $l_1$  minimization," *Journal of Fourier analysis and applications*, vol. 14, no. 5-6, pp. 877–905, 2008.
- [14] R. Chartrand and W. Yin, "Iteratively reweighted algorithms for compressive sensing," in *Acoustics, speech and signal processing, 2008. ICASSP 2008. IEEE international conference on*. IEEE, 2008, pp. 3869–3872.
- [15] F. Li, R. Xie, W. Song, T. Zhao, and K. Marfurt, "Optimal  $l_q$  norm regularization for sparse reflectivity inversion," in *SEG Technical Program Expanded Abstracts 2017*. Society of Exploration Geophysicists, 2017, pp. 677–681.
- [16] R. Zhang, K. Zhang, and J. E. Alekhue, "Depth-domain seismic reflectivity inversion with compressed sensing technique," *Interpretation*, vol. 5, no. 1, pp. T1–T9, 2016.
- [17] L. P. de Figueiredo, M. Santos, M. Roisenberg, G. S. Neto, and W. Figueiredo, "Bayesian framework to wavelet estimation and linearized acoustic inversion," *IEEE Geoscience and Remote Sensing Letters*, vol. 11, no. 12, pp. 2130–2134, 2014.
- [18] R. Tibshirani, "Regression shrinkage and selection via the lasso," *Journal of the Royal Statistical Society. Series B (Methodological)*, pp. 267–288, 1996.
- [19] L. E. Frank and J. H. Friedman, "A statistical view of some chemometrics regression tools," *Technometrics*, vol. 35, no. 2, pp. 109–135, 1993.
- [20] Y. Sun, P. Babu, and D. P. Palomar, "Majorization-minimization algorithms in signal processing, communications, and machine learning," *IEEE Transactions on Signal Processing*, vol. 65, no. 3, pp. 794–816, 2017.
- [21] S. Arlot, A. Celisse *et al.*, "A survey of cross-validation procedures for model selection," *Statistics surveys*, vol. 4, pp. 40–79, 2010.